Journal of Statistical Physics, Vol. 13, No. 2, 1975

A Lattice Model for a Real Substance

H. P. Neumann

Received August 16, 1973; revised December 11, 1974

A linear, a plane square, and a simple cubic hard core lattice model are treated by a mean-field approximation combined with a combinatorial approach. Assuming a hard core interaction between nearest-neighbor lattice sites and a rather arbitrary soft pair interaction between lattice sites placed at longer distances from one another, inert-gas-like phase diagrams can be constructed for suitable chosen combinatorial ansatzes.

KEY WORDS : Hard core lattice model ; mean-field approximation ; quasi-chemical approximation ; modified quasichemical approximation ; state equations ; phase diagrams.

1. INTRODUCTION

The thermodynamic properties of fluids and crystals can be understood in terms of a statistical mechanical lattice model consisting of a great (infinite) number of classical particles moving from site to site on a very large (infinite) regular lattice after the laws of classical mechanics. The interaction between the particles is thereby considered in general as a pair interaction, which consists of a short-ranged hard core with a soft interaction tail of arbitrary range.[1-34]

In a preceding paper,[39] referred to hereafter as paper I, we investigated a classical system of particles on a linear, on a plane square, and on a three-dimensional simple cubic lattice with a hard core interaction extending up to the first nearest-neighbor shell and an arbitrary soft pair interaction $-v_{ij}$ of infinite range but with a finite total interaction energy per lattice site $-v$.

[1] Institut für Physikalische Chemie der Universität Frankfurt, Frankfurt/Main, Germany.

© 1975 Plenum Publishing Corporation, 227 West 17th Street, New York, N.Y. 10011. No part of this publication may be reproduced, stored in a retrieval system, or transmitted, in any form or by any means, electronic, mechanical, photocopying, microfilming, recording, or otherwise, without written permission of the publisher.

Treating the part of the grand canonical partition function that is governed by the soft interaction tail in mean-field approximation and the hard core part in Kikuchi's quasichemical (QC) approximation,[35] the existence of at most three stable phases—a gas phase, a liquid phase, and a crystalline phase with close-packed periodic structure—could be proved for each of the three lattice types. It has also been shown that the three phases can undergo gas–liquid and fluid–solid phase transitions of first order.

On the other hand, a realistic pressure–temperature phase diagram, which exhibits the characteristics of a real gas–liquid–solid phase diagram as known from inert gases,[38] could be calculated only by assuming a suitable functional dependence between the geometrical structure of the interaction and the temperature. (See Fig. 9 in I.)

In the present paper[2] it will be shown how, by a somewhat more general combinatorial approach using the combinatorial factor[39] $W_{\mathrm{HC}}(\rho_1, \rho_2)$, which may be called a modified quasichemical (MQC) approximation, a still greater agreement of the theoretical results for these models with experimental data can be reached.

2. DERIVATION OF STATE EQUATIONS AND THEIR SOLUTION

The hard core correlation in our lattice models is transferred only by nearest-neighbor links. It therefore appears reasonable to reduce the calculation of $W_{\mathrm{HC}}(\rho_1, \rho_2)$, which is the number of compatible hard core configurations with fixed sublattice densities ρ_1, ρ_2 on our lattices with coordination number z, which are composed of a black sublattice 1 and a white sublattice 2 each consisting of $V/2$ lattice sites (see Fig. 1a), to a counting of configuration numbers

$$Q(c, (zV/2)\langle p^{(2)}\rangle(k)), \qquad Q(b, (V/2)\langle p^{(11)}\rangle(k), (V/2)\langle p^{(12)}\rangle(k))$$

and

$$Q(d, (zV/2)\langle p^{(11)}\rangle(k), (zV/2)\langle p^{(12)}\rangle(k))$$

on certain pseudolattices c, b, d according to the ansatz[36,37]

$$W_{\mathrm{HC}}(\rho_1, \rho_2) = Q(c, (zV/2)\langle p^{(2)}\rangle(k)) \times \left[\frac{Q(b, (V/2)\langle p^{(11)}\rangle(k), (V/2)\langle p^{(12)}\rangle(k))}{Q(d, (zV/2)\langle p^{(11)}\rangle(k), (zV/2)\langle p^{(12)}\rangle(k))}\right]^{1/\alpha(\rho_1,\rho_2)} \tag{1}$$

Thus $Q(m, \{x_{lh}(m)V\langle p^{(lh)}\rangle(k)\})$ is generally the number of configurations on a

[2] Parts of this work and of Ref. 39 have been presented at the Spring Meetings of the Deutsche Physikalische Gesellschaft in Münster (19–24 March 1973) and of the Bunsengesellschaft für Physikalische Chemie in Erlangen (31 May–2 June 1973).

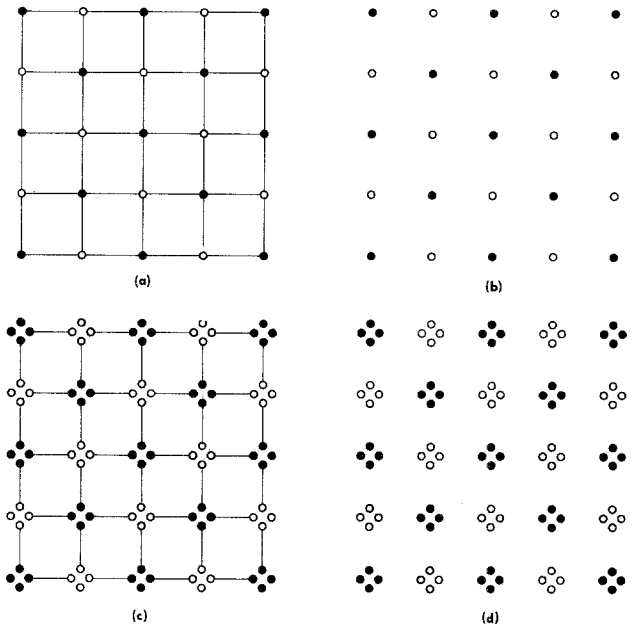

Fig. 1. Pseudolattices produced by successive intersection of a plane square lattice composed of two equivalent sublattices.

pseudolattice m consisting of $x_{lh}(m)V$ uncorrelated lattice site subsets of type lh built up by l lattice sites in the way h, where the lattice site subsets lh, which are occupied by only one or no particle in the way k, occur with the fixed probability $\langle p^{(lh)}\rangle(k)$. The pseudolattices c, b, d, which must be considered only in the case of our models, consist of $zV/2$ uncorrelated nearest-neighbor links (Fig. 1c) and $V/2$ or $zV/2$ uncorrelated black and white lattice sites (Figs. 1b, 1d), respectively.

The $\alpha(\rho_1, \rho_2)$ in (1) can be assumed in general to be an arbitrary positive function, which varies probably slowly in a wide region of the ρ_1, ρ_2 domain.

The configuration numbers $Q(m, \{x_{lh}(m)V\langle p^{(lh)}\rangle(k)\})$ on the pseudo lattices can be counted easily by the formula

$$Q(m, \{x_{lh}(m)V\langle p^{(lh)}\rangle(k)\}) = \prod_h \prod \frac{(x_{lh}(m)V)!}{\prod_k (x_{lh}(m)V\langle p^{(lh)}\rangle(k))!} \tag{2}$$

where in $Q(c, (zV/2)\langle p^{(2)}\rangle(k))$ the correct probabilities $\langle p^{(2)}\rangle(k)$ of the subfigures listed in Fig. 2 must be inserted, while in $Q(b, (V/2)\langle p^{(11)}\rangle(k)$, $(V/2)\langle p^{(12)}\rangle(k))$ and $Q(d, (zV/2)\langle p^{(11)}\rangle(k)$, $(zV/2)\langle p^{(12)}\rangle(k))$, $\langle p^{(1h)}\rangle(1) = \rho_h$ and $\langle p^{(1h)}\rangle(2) = 1 - \rho_h$ can be used.

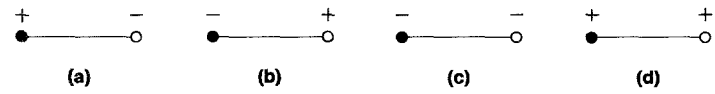

Fig. 2. Basic subdiagrams on a periodically occupied rectangular lattice, with the mean occupation numbers (a) $\langle p^{(2)}\rangle(1) = \rho_1$, (b) $\langle p^{(2)}\rangle(2) = \rho_2$, (c) $\langle p^{(2)}\rangle(3) = 1 - \rho_1 - \rho_2$, (d) $\langle p^{(2)}\rangle(4) = 0$. The plus sign means occupation by a particle, while the minus sign means occupation by a hole.

Because $\alpha(\rho_1, \rho_2)$ in (1) is a comparatively arbitrary function, there are many possibilities for approximate calculations of $W_{\mathrm{HC}}(\rho_1, \rho_2)$, but the suggestion that $\alpha(\rho_1, \rho_2)$ is a slowly varying function justifies taking in a first approximation α in (1) simply as a variable parameter.

The corresponding mean-field state equations[39] calculated with the aid of (1) and (2) are then

$$\begin{aligned} p = \tfrac{1}{4}\{&v(1)(\rho_1)^2 + v(2)(\rho_2)^2 + v(12)\rho_1\rho_2 + v(21)\rho_2\rho_1 \\ &+ 2(\rho_1 + \rho_2)\mu + (2/\alpha\beta)[(z-1)(1-\rho_1)\ln(1-\rho_1) \\ &+ (z-1)(1-\rho_2)\ln(1-\rho_2) \\ &- [z(\alpha-1)+1]\rho_1 \ln \rho_1 - [z(\alpha-1)+1]\rho_2 \ln \rho_2 \\ &- \alpha z(1-\rho_1-\rho_2)\ln(1-\rho_1-\rho_2)]\} \end{aligned} \tag{3}$$

$$\frac{(1-\rho_1)^{z-1}(\rho_1)^{z(\alpha-1)+1}}{(1-\rho_1-\rho_2)^{\alpha z}} = \exp\{\alpha\beta[v(1)\rho_1 + v(12)\rho_2 + \mu]\} \tag{4}$$

$$\frac{(1-\rho_2)^{z-1}(\rho_2)^{z(\alpha-1)+1}}{(1-\rho_1-\rho_2)^{\alpha z}} = \exp\{\alpha\beta[v(2)\rho_2 + v(21)\rho_1 + \mu]\} \tag{5}$$

where p is the pressure; $\beta = 1/kT$, with k Boltzmann's constant and T the absolute temperature; and μ is the chemical potential.

The interaction terms $v(1)$ and $v(2)$ are the total negative interaction energies per lattice site on the sublattices 1 and 2. The terms $v(r, s)$ represent the total negative interaction energy between one lattice site i of the sublattice r with all the other lattice sites of sublattice s that are not nearest neighbors of i.

The terms $v(1)$, $v(2)$, $v(12)$, and $v(21)$ can be easily expressed in terms of v and an interaction structure parameter $\bar{v}$, defined by

$$\bar{v} = (1/v)[v(1) - v(12)] = (1/v)[v(2) - v(21)] \tag{6}$$

One recognizes that $\alpha = 1$ yields the QC state equations of paper I. This corresponds to an approximation considered previously for fluid phases.[36,37]

The state equations (4) and (5) can be solved now by the same method as employed in paper I. A detailed investigation shows that solutions of (4) and (5) that are not unreasonable can be obtained only for values of α with

$z(\alpha - 1) + 1 > 0$. For these values of α, as in paper I, a homogeneous solution $\rho_1 \equiv \rho_2$ of (4) and (5) is found, which describes partially a stable gas phase g and partially a stable liquid phase l. Further, an inhomogeneous solution $\rho_1 > \rho_2$ is found describing a stable solid phase s. Corresponding density and pressure state isotherms similar to that in paper I can be constructed. The homogeneous solution of (4) and (5) thus exhibits only a weak dependence on α.

The contrary is true for the behavior of the inhomogeneous solution of (4) and (5). A complete solution of (4) and (5) shows that in the following cases

(a) $z(\alpha - 2) + 2 \geqslant 0$
(b) $z(\alpha - 2) + 2 \leqslant 0, \quad \alpha > \alpha^*$
(c) $z(\alpha - 1) + 1 > 0, \quad \alpha < \alpha^*$

essentially different solid state isotherms and fluid–solid phase transition curves result [α^* is the value of α for which the higher density zero of the denominator in (8) coincides with the zero of f_1 from (9)].

For a better illustration the pseudo-critical density ρ_{cgs} as a function of the interaction structure parameter $\bar{v}$ is given in Fig. 3 and complete pressure–temperature phase diagrams are shown in Figs. 4–7.

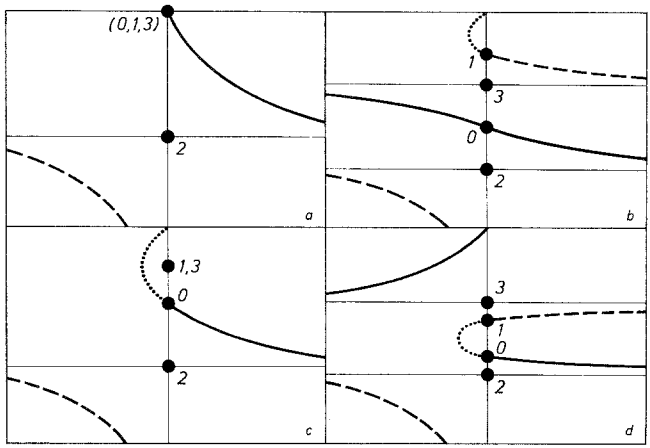

Fig. 3. Densities ρ_{cgs} vs. $\bar{v}$ calculated from (7)–(9). Regions of coordinates: $0 \leqslant \rho_{cgs} \leqslant 0.5$; $-\infty < \bar{v} < \infty$. Part (a) is valid for $z(\alpha - 2) + 2 \geqslant 0$; (b) is valid for $z(\alpha - 2) + 2 < 0$, $\alpha > \alpha^*$; (c) is valid for $\alpha = \alpha^*$; (d) is valid for $\alpha < \alpha^*$, $z(\alpha - 1) + 1 > 0$. The solid curves correspond to a soft interaction tail with $v > 0$, the dashed curves to an interaction with $v < 0$. The numbers 0, 1 indicate the zeros of f_0 and f_1 in (9), and 2, 3 indicate the zeros of the denominator of (8) with lower and higher density. The (0, 1, 3) in (a) is only valid for $z(\alpha - 2) + 2 = 0$. At $\rho_{cgs} = 0$ we always have $\bar{v} = -2$.

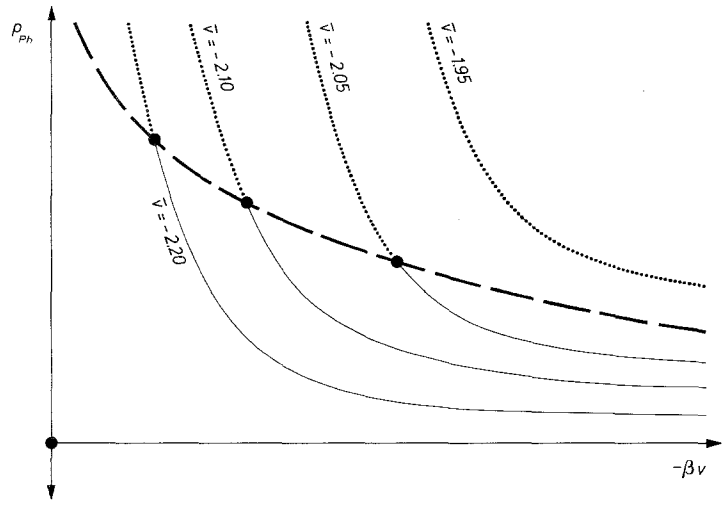

Fig. 4. Pressure–temperature (p_{Ph}–βv) phase diagram for the coexistence curves of a lattice system with a mean repulsive soft particle interaction ($v < 0$) for the case $v\bar{v} > 0$, $z(\alpha - 2) + 2 > 0$.

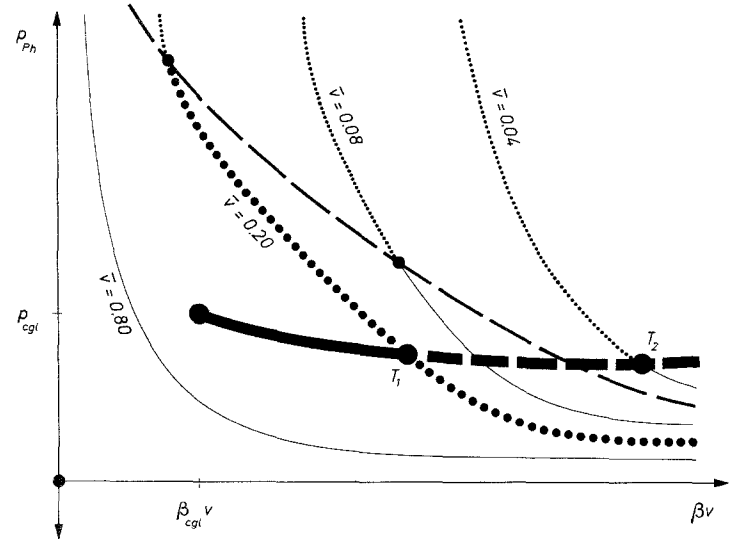

Fig. 5. Pressure–temperature (p_{Ph}–βv) phase diagram for the coexistence curves of a lattice system with a mean attractive soft particle interaction ($v > 0$) for the case $v\bar{v} > 0$, $z(\alpha - 2) + 2 > 0$.

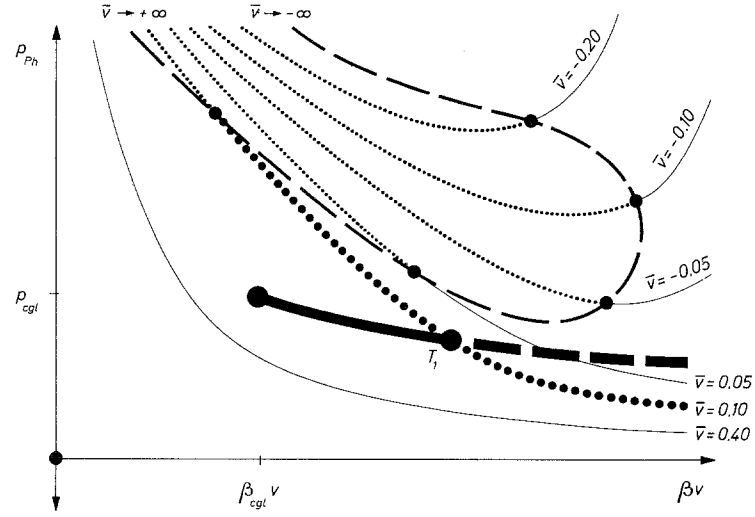

Fig. 6. Pressure–temperature (p_{Ph}–βv) phase diagram for the coexistence curves of a lattice system with mean attractive soft particle interactions ($v > 0$) of types $v\bar{v} \gtrless 0$ in the case $z(\alpha - 2) + 2 < 0$, $|z(\alpha - 2) + 2| \ll 1$.

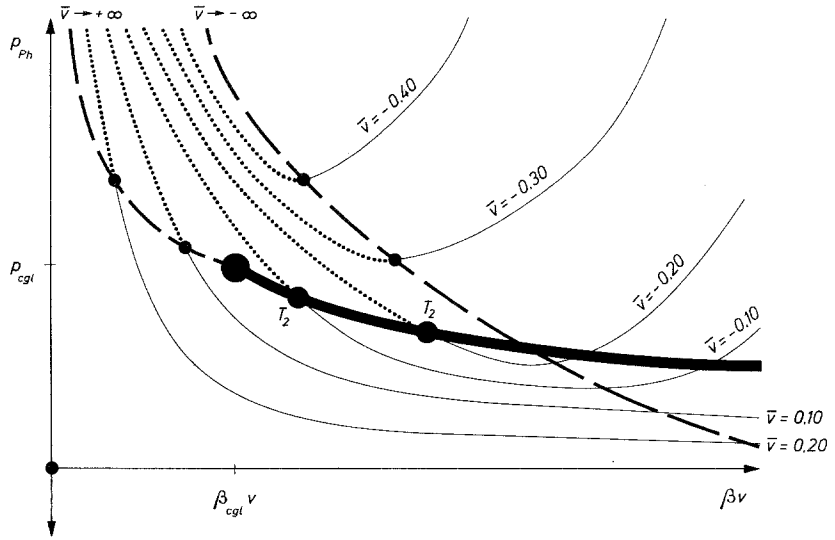

Fig. 7. Pressure–temperature (p_{Ph}–βv) phase diagram for the coexistence curves of a lattice system with mean attractive soft particle interactions ($v > 0$) of types $v\bar{v} \gtrless 0$ in the case $\alpha < \alpha^*$, $z(\alpha - 1) + 1 > 0$.

The pseudo-critical points of the fluid–solid transition are characterized by a change of the first-order fluid–solid transition into a continuous order–disorder transition. These critical points have very little in common with the gas–liquid critical point marked with the index *cgl* in Figs. 5–7. Therefore they may be called pseudo-critical points. The pseudo-critical density ρ_{cgs} and the pseudo-critical temperature $1/k\beta_{cgs}$ are determined by the equations

$$\beta_{cgs}v\bar{v} = \frac{1}{2\alpha}\frac{f_0}{\rho_{cgs}(1-\rho_{cgs})} \tag{7}$$

$$\bar{v} = (1-2\rho_{cgs})f_0f_1\{4\alpha z\rho_{cgs}(1-\rho_{cgs})f_1 + (1-2\rho_{cgs})[f_0f_1+3(f_2)^2]\}^{-1} \tag{8}$$

The f_0, f_1, and f_2 in (7) and (8) are the following functions:

$$\begin{aligned} f_0(\rho_{cgs}) &= z(\alpha-2)+2+\alpha z(1-2\rho_{cgs}) \\ f_1(\rho_{cgs}) &= (z-1)(\rho_{cgs})^3 - [z(\alpha-1)+1](1-\rho_{cgs})^3 \\ f_2(\rho_{cgs}) &= (z-1)(\rho_{cgs})^2 + [z(\alpha-1)+1](1-\rho_{cgs})^2 \end{aligned} \tag{9}$$

The various lines in Figs. 4–7 have the following meanings: The heavy, partially solid, partially dashed lines represent condensation curves. The groups of thin, partially solid, partially dotted lines with the parameter $\bar{v}$ represent fluid–solid transition curves. The parts of the fluid–solid transition curves that lie above a condensation curve represent for gas–liquid subcritical temperatures the fluid–solid transition of a three-phase gas–liquid–solid system. All other parts represent the fluid–solid transition of two-phase fluid–solid systems. In Figs. 5–7 the fluid–solid transition curves intersect the condensation curves for smaller values of $|\bar{v}|$ in triple points of types T_1 and T_2.

The triple points T_1 in Figs. 5 and 6 are realistic, while the triple points T_2 in Fig. 5 and 7 are pseudo-critical points. They are not very realistic because for higher temperatures only a continuous order–disorder fluid–solid transition exists.

The continuous parts of the thin fluid–solid transition curves are due to first-order transitions. The dotted parts describe the continuous order–disorder transitions. Both parts are separated by the thinner dashed curves in Figs. 4–7,[3] which are calculated by (7)–(9) and correspond to the curves in Fig. 3. In the case $v > 0$ this is only true in the βv regions where the dashed curves lie above the heavy condensation curves.

In Figs. 5–7 the thinner dashed curves intersect the heavy condensation curves and lie below these curves at lower temperatures. For these tempera-

[3] The dashed curves have high-pressure asymptotes $p(\bar{v} = \pm\infty) = +\infty$, $\beta v(\bar{v} = \pm\infty) = 0$ and low-pressure asymptotes $p(\bar{v} = -2) = 0$, $\beta v(\bar{v} = -2) = -\infty$ (in Fig. 4) and $p\ (\bar{v} = 0) = -\frac{1}{2}v(\rho_{cgs})^2$, $|\beta v(\bar{v} = 0)| = \infty$ (in Figs. 5 and 7).

tures the pseudo-critical curves are identical with the condensation curves and *not* with the thinner dashed lines.

The fluid–solid transition curves with $v\bar{v} > 0$ in Figs. 4 and 5 have asymptotes at temperatures defined by

$$\beta v\bar{v} = 2[z(\alpha - 2) + 2]/\alpha \tag{10}$$

while the fluid–solid transition curves in Figs. 6 and 7 have one common asymptote at $\beta v = 0$ for both $v\bar{v} \gtrless 0$, and for $v\bar{v} < 0$ have asymptotes defined by

$$\beta v\bar{v} = (4/\alpha)[z(\alpha - 2) + 2] \ln 2 \tag{11}$$

For predominantly attractive soft interactions with smaller values of $\bar{v}$, Fig. 5 up to medium temperatures and Fig. 6 for the whole range of temperatures show the existence of quite realistic fluid–solid transition curves. Such curves are drawn in Figs. 5 and 6 as heavy dotted lines, yielding, together with the continuous parts of the condensation curves, realistic inert-gas-like phase diagrams. The dashed parts of the condensation curves then represent fictitious parts, because in this range of temperature, liquid phases are not stable. In Fig. 5, $\bar{v}$ is not allowed to become too small, otherwise unrealistic triple points of type T_2 will occur.

Although the phase diagrams in case (a) of the MQC approximation (Figs. 4 and 5) are in fair agreement up to moderately high pressures and temperatures with experimental data for soft interactions with $v\bar{v} > 0$, they are nevertheless unsatisfactory for high pressures, high temperatures, and in the limit $v \to 0$. For high pressures the course of the fluid–solid transition curves becomes wrong. For high temperatures and in the limit $v \to 0$ only fluid phases can occur, in contradiction to other theoretical results.[4–30]

A further shortcoming is the nonexistence of a solid phase for soft interactions with $v\bar{v} < 0$ in the whole range of temperature. Obviously the combinatorial approach for $W_{\mathrm{HC}}(\rho_1, \rho_2)$ of case (a) is not very suitable, but the shortcomings can be compensated partially by the mean-field treatment of the soft interaction tail at least for interactions with $v\bar{v} > 0$.

In case (c) of the MQC approximation the shortcomings of case (a) of the MQC approximation are absent. This is underlined by the course of the fluid–solid transition curves in Fig. 7. But unfortunately the triple points T_2 and the nature of the fluid–solid transitions for temperatures above the triple points T_2 are not very realistic.

All the imperfections of the MQC approximations (a) and (c) are removed in the case of the MQC approximation of type (b). A typical phase diagram for a predominantly repulsive soft interaction ($v < 0$), which is also valid in case (c), is shown in Fig. 8 of paper I. Characteristic phase diagrams for predominantly attractive soft interactions ($v > 0$) are represented by

Fig. 6 of this paper and Fig. 7 of paper I. They are in fair agreement with results of Runnels,[26] who treated the same hard core lattice models considering short-ranged soft interactions with $v \gtrless 0$, $\bar{v} = 1$.

As demonstrated by the phase diagram of Fig. 6, the MQC approach of type (b) is most suitable for describing experimental data, especially in the case $|z(\alpha - 2) + 2| \ll 1$. In this case for small $\bar{v}$ realistic complete pressure–density state diagrams according to Fig. 6 can be drawn like that represented by Fig. 10 in paper I.

Phase diagrams calculated in the QC approximation, such as Fig. 7 in paper I, are more in agreement with results of Stell *et al.*,[33,34] who treated our hard core lattice models in the case of long-ranged soft interactions, so-called Kac potentials with $v > 0$, $\bar{v} = 0$. The unrealistic high-pressure asymptotes of the fluid–solid transition curves at lower temperatures in the case $v\bar{v} < 0$ could not be removed by the MQC approximations. They are probably caused by the imperfection of the mean-field approach.

REFERENCES

1. A. Münster, *Statistical Thermodynamics*, Vol. I (Academic Press, New York, 1969) and references cited therein.
2. T. D. Lee and C. N. Yang, *Phys. Rev.* **87**:410 (1952).
3. C. Domb and M. F. Sykes, *Advan. Phys.* **9**:245 (1960).
4. B. J. Alder and T. E. Wainwright, *J. Chem. Phys.* **33**:1439 (1960).
5. B. J. Alder and T. E. Wainwright, *Phys. Rev.* **127**:359 (1962).
6. W. W. Wood and J. D. Jacobson, *J. Chem. Phys.* **27**:1207 (1957).
7. W. W. Wood, F. R. Parker, and J. D. Jacobson, *Nuovo Cimento* **9** (Suppl. 1):133 (1958).
8. C. Domb, *Nuovo Cimento* **9**(Suppl. 1):9 (1958).
9. H. N. V. Temperley, *Proc. Phys. Soc. (London) A* **67**:233 (1954).
10. H. N. V. Temperley, *Proc. Phys. Soc. (London) B* **70**:536 (1957).
11. H. N. V. Temperley, *Proc. Phys. Soc. (London)* **74**:183, 432 (1959).
12. H. N. V. Temperley, *Proc. Phys. Soc. (London) B* **77**:630 (1961).
13. H. N. V. Temperley, *Proc. Phys. Soc. (London)* **80**:813, 823 (1962).
14. D. M. Burley, *Proc. Phys. Soc. (London)* **75**:262 (1960).
15. D. M. Burley, *Proc. Phys. Soc. (London)* **77**:451 (1961).
16. D. M. Burley, *Proc. Phys. Soc. (London) B* **85**:1173 (1965).
17. D. S. Gaunt and M. E. Fisher, *J. Chem. Phys.* **43**:2840 (1965).
18. F. H. Ree and D. A. Chesnut, *J. Chem. Phys.* **45**:3983 (1966).
19. L. K. Runnels and L. L. Combs, *J. Chem. Phys.* **45**:2482 (1966).
20. L. K. Runnels, *Phys. Rev. Lett.* **15**:581 (1965).
21. L. K. Runnels, *J. Math. Phys.* **8**:2081 (1967).
22. F. H. Ree and D. A. Chestnut, *Phys. Rev. Lett.* **18**:5 (1967).
23. D. S. Gaunt, *J. Chem. Phys.* **46**:3237 (1967).
24. A. Bellemans and R. K. Nigam, *J. Chem. Phys.* **46**:2922 (1967).
25. J. Orban and A. Bellemans, *J. Chem. Phys.* **49**:363 (1968).
26. L. K. Runnels, *J. Math. Phys.* **11**:842 (1970).
27. L. K. Runnels, J. P. Salvant, and H. R. Streiffer, *J. Chem. Phys.* **52**:2352 (1970).

28. L. K. Runnels, J. R. Craig, and H. R. Streiffer, *J. Chem. Phys.* **54**:2004 (1971).
29. J. Orban, J. v. Craen, and A. Bellemans, *J. Chem. Phys.* **49**:1778 (1968).
30. W. G. Hoover, B. J. Alder, and F. H. Ree, *J. Chem. Phys.* **41**:3528 (1964).
31. J. L. Lebowitz and O. Penrose, *J. Math. Phys.* **7**:98 (1966).
32. D. J. Gates and O. Penrose, *Commun. Math. Phys.* **15**:255 (1966).
33. G. Stell, H. Narang, and C. K. Hall, *Phys. Rev. Lett.* **28**:292 (1972).
34. C. K. Hall and G. Stell, *Phys. Rev. A* **7**:1679 (1973).
35. R. Kikuchi, *Phys. Rev.* **81**:988 (1951).
36. J. Hijmans and J. de Boer, *Physica* **21**:471–516 (1955).
37. F. E. J. Kruseman Aretz and E. G. D. Cohen, *Physica* **26**:967 (1960).
38. G. A. Cook, *Argon, Helium and the Rare Gases*, Vol. I (Interscience, New York, 1961).
39. H. P. Neumann, *Z. Naturforsch.* **29a**:65 (1974).